NBSIR 79–1615

DISPERSION AND ATTENUATION CHARACTERISTICS OF MODES IN A TEM–CELL WITH A LOSSY DIELECTRIC SLAB

John C. Tippet
David C. Chang

Department of Electrical Engineering
University of Colorado
Boulder, Colorado 80309

Sponsored by:
Electromagnetic Fields Division
National Engineering Laboratory
National Bureau of Standards
Boulder, Colorado 80303

August 1979

NBSIR 79–1615

DISPERSION AND ATTENUATION CHARACTERISTICS OF MODES IN A TEM–CELL WITH A LOSSY DIELECTRIC SLAB

John C. Tippet
David C. Chang

Department of Electrical Engineering
University of Colorado
Boulder, Colorado 80309

Sponsored by:
Electromagnetic Fields Division
National Engineering Laboratory
National Bureau of Standards
Boulder, Colorado 80303

August 1979

U.S. DEPARTMENT OF COMMERCE, Juanita M. Kreps, Secretary
Luther H. Hodges, Jr., Under Secretary
Jordan J. Baruch, Assistant Secretary for Science and Technology

NATIONAL BUREAU OF STANDARDS, Ernest Ambler, Director

CONTENTS

FOREWORD

This report describes a theoretical analysis developed by the staff of the University of Colorado at Boulder under a contract sponsored by the National Bureau of Standards (NBS). Professor David C. Chang of the Electromagnetic Laboratory heads the University team. Mark T. Ma of the NBS Electromagnetic Fields Division serves as the current technical contract monitor.

The work included in this report represents a further aspect of theoretical analyses of Transverse Electromagnetic (TEM) Transmission Line cells developed at NBS. The purpose of this effort is to evaluate the use of TEM cells for (i) measuring the total rf power radiated by a device inserted into the cell for test, or (ii) performing necessary susceptibility tests on a small electronic device.

Previous results indicate that the useful frequency range of such TEM cells is limited by the possible presence of higher-order modes. It has been suggested that the useful frequency range may be extended by loading the cell with an absorbing material or a lossy dielectric slab. In this report, the problem of loading the lower half of the cell with a lossy dielectric slab is formulated with coupled integral equations. The position of the center septum inside the cell is not restricted. Dispersion and attenuation characteristics of the dominant mode as well as of the higher-order modes are investigated. Numerical results are also included. It is found that while an insertion of a lossy material can indeed lower the Q-factor of the higher order modes and thus help extend the useful frequency range, it also attenuates the dominant mode. Therefore, an appropriate correction factor to this effect must be considered before trying to predict radiation/susceptibility results in a free-space environment based on the measured data taken inside the cell.

Previous publications under the same effort include:

J. C. Tippet and D. C. Chang, Radiation characteristics of dipole sources located inside a rectangular coaxial transmission line, NBSIR 75-829, January 1976.

J. C. Tippet, D. C. Chang and M. L. Crawford, An analytical and experimental determination of the cut-off frequencies of higher-order TE modes in a TEM cell, NBSIR 76-841, June 1976.

J. C. Tippet and D. C. Chang, Higher order modes in rectangular coaxial line with infinitely thin inner conductor, NBSIR 78-873, March 1978.

I. Sreenivasiah and D. C. Chang, A variational expression for the scattering matrix of a coaxial line step discontinuity and its application to an over moded coaxial TEM cell, NBSIR 79-1606, May 1979.

DISPERSION AND ATTENUATION CHARACTERISTICS OF MODES IN A TEM-CELL WITH A LOSSY DIELECTRIC SLAB

Dispersion and attenuation characteristics of the dominant mode in a TEM cell, loaded with a lossy dielectric slab, are investigated. It is shown that, while the insertion of the lossy material can indeed lower the Q-factor of the higher-order modes, the attenuation of the dominant mode also increases drastically as frequency increases. Correction to that effect must be taken before measurements in the cell are used to correlate to those taken in a free-space environment.

Key words: Attenuation; coupled integral equations; dispersion; lossy dielectric slab; modes considerations; TEM-cell.

1. INTRODUCTION

It has been suggested that in the design of a TEM-cell, a loading of the cell with absorbing material is sometimes desirable in reducing the Q-factor of the higher-order modes and thus, can extend the useful frequency range [1]. Since the absorbing material also perturbs the distribution of the dominant mode and causes additional attenuation, such an arrangement will certainly complicate the correction factor one seeks to relate measurements within the TEM cell and those taken in a free-space environment. Thus, our aim in this report is to investigate theoretically the dispersion as well as attenuation characteristics of the dominant mode in the case when the lower half of the cell is lined with a lossy dielectric slab. The structure resembles that of a shielded stripline which is extensively investigated in the literature, with the only exception that the strip (or center septum) is now elevated instead of lying on the dielectric interface.

In early analyses of the stripline problem [2], the dominant mode of propagation was usually assumed to be a pure TEM mode. The justification was made that for high dielectric constants and low frequencies, the field was mainly confined in the dielectric layer; thus, approximate solutions could be obtained using conformal transformation methods. Recently, more rigorous solutions have appeared which involve expansions in terms of hybrid modes. These solutions are generally not restricted to the low frequency range, and in some cases data are presented for the propagation constants of higher-order modes. Most of these analyses begin with a coupled-integral-equation formulation. The method of solution of the resulting integral equations distinguishes the various approaches to the problem which can be roughly divided into three categories: (1) finite difference or finite element methods [3-5], (2) generalized moment methods [6-12], and (3) the singular integral equation method [13-15]. The approach taken in this work is one based on the singular integral equation method developed in our earlier report [16]; thus, it would fall into the last category mentioned above. In common with the other singular integral equation approaches, this method enables one to obtain accurate values for the propagation constants by inverting relatively small-order matrices (as compared to categories (1) and (2)). There are some important differences in our approach, however, and these can be summarized as follows: (1) since we have not assumed a symmetrically located inner conductor, we do not restrict our solution to modes with even symmetry, (2) the location of the inner conductor is not restricted to the dielectric interface, (3) we have used a dual formulation in terms of the currents on the inner conductor rather than the fields in the gap region, and (4) the nonsingular kernel is expanded in terms of Chebyshev polynomials which leads to a set of canonical integrals which can be evaluated in closed-form in terms of complete elliptic integrals. The asymptotic forms of these elliptic integrals for modulus near zero or one can then be used to obtain approximate secular equations valid in the narrow-strip or small gap regions. Cross section of the device is shown in Fig. 1. This structure consists of a Rectangular Cross Section Transmission Line which is loaded with a layer of dielectric material. The dielectric layer is modeled by region 1 and is assumed to have a complex relative permittivity ε_r, permeability μ_r, while those of the remaining regions are assumed to be unity.

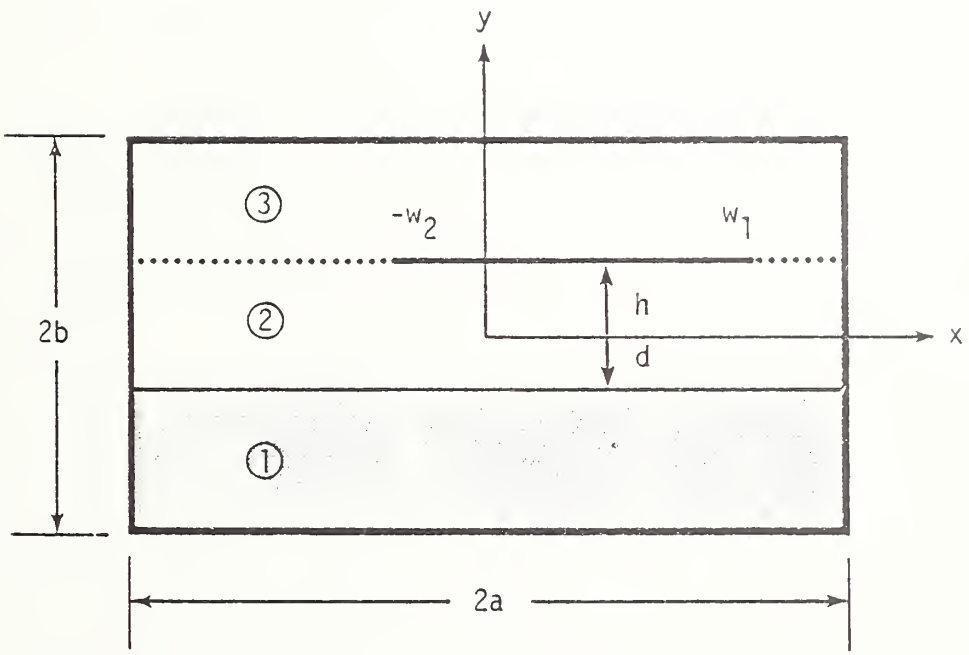

Figure 1. Cross-section of a TEM-cell with a dielectric slab

2. COUPLED INTEGRAL EQUATION FORMULATION FOR THE CURRENTS ON THE INNER CONDUCTOR

Since we know that the modes in this type of structure are not pure TE or TM modes, it is convenient to formulate the problem in terms of hybrid modes. In the absence of the inner conductor, we know that the modes are just the LSE or LSM modes of a partially-filled rectangular waveguide; thus these modes are naturally suited as basis functions in the formulation. In order to match the boundary conditions at the inner conductor, a superposition of both the LSE and LSM modes is required. This can be accomplished by expressing the fields in terms of two Hertz vectors directed normal to the dielectric interface. Assuming propagation according to the factor $e^{j\omega t-\Gamma z}$ we find that the fields in each region (n=1,2,3) can be expressed in terms of the LSE, LSM potentials as follows:

$$\bar{E}_n = \nabla \times \nabla \times \bar{\Phi}_n - j\omega\mu_n \nabla \times \bar{\Psi}_n \tag{1}$$

and

$$\bar{H}_n = j\omega\varepsilon_n \nabla \times \bar{\Phi}_n + \nabla \times \nabla \times \bar{\Psi}_n \tag{2}$$

where

$$\bar{\Phi}_n = \bar{a}_y \, \phi_n(x,y) \ , \tag{3}$$

$$\bar{\Psi}_n = \bar{a}_y \, \psi_n(x,y) \ , \tag{4}$$

and ϕ_n and ψ_n satisfy the wave equation:

$$[\nabla_t^2 + (\Gamma^2 + k_n^2)] \begin{pmatrix} \phi_n \\ \psi_n \end{pmatrix} = 0 \tag{5}$$

with

$$k_n = \omega[\mu_n \varepsilon_n]^{\frac{1}{2}} \quad .$$

In the above equations ε_n and μ_n are respectively the dielectric permittivity and magnetic permeability of each region and ∇_t^2 is the transverse Laplacian given by

$$\nabla_t^2 = \partial_{xx} + \partial_{yy} \quad .$$

The six field components in each region can be found by substituting (3) and (4) into (1) and (2) with the following result:

$$E_{xn} = -jk_n\zeta_n\Gamma\psi_n + \partial_{xy}\phi_n \quad , \tag{6}$$

$$E_{yn} = -(\partial_{xx} + \Gamma^2)\phi_n \quad ,$$

$$E_{zn} = -jk_n\zeta_n\partial_x\psi_n - \Gamma\partial_y\phi_n \quad , \tag{7}$$

$$H_{xn} = \partial_{xy}\psi_n + j\frac{k_n}{\zeta_n}\Gamma\phi_n \quad ,$$

$$H_{yn} = -(\partial_{xx} + \Gamma^2)\psi_n \quad ,$$

and

$$H_{zn} = -\Gamma\partial_y\psi_n + j\frac{k_n}{\zeta_n}\partial_x\phi_n \quad ,$$

where

$$\zeta_n = [\mu_n/\epsilon_n]^{\frac{1}{2}} \quad .$$

The scalar potentials ϕ_n and ψ_n are found by solving (5) subject to the boundary conditions on the metal walls. The appropriate expansions to use are given as follows:

$$\phi_n = \sum_{m=0}^{\infty} A_{mn} \sin \sigma_m(x+a) \cosh \gamma_{mn} (y \pm b) \ , \ n=1,3 \ , \tag{8}$$

$$\psi_n = \sum_{m=0}^{\infty} B_{mn} \cos \sigma_m(x+a) \sinh \gamma_{mn} (y \pm b) \ , \ n=1,3 \ , \tag{9}$$

$$\phi_2 = \sum_{m=0}^{\infty} A_{m2} \sin \sigma_m(x+a) \cosh \gamma_{mo}(y+d) \ [1+R_{m2} \tanh \gamma_{mo}(y+d)] \ ,$$

$$\psi_2 = \sum_{m=0}^{\infty} B_{m2} \cos \sigma_m(x+a) \cosh \gamma_{mo}(y+d) \ [1+S_{m2} \tanh \gamma_{mo}(y+d)] \ ,$$

where

$$\sigma_m = \frac{m\pi}{2a} \ ,$$

$$\gamma_{mn} = [\sigma_m^2 - \Gamma^2 - k_n^2]^{\frac{1}{2}} \ ,$$

$$k_3 = k_o \ ,$$

and A_{mn}, B_{mn}, R_{m2} and S_{m2} are expansion coefficients yet to be determined. In (8) and (9) the upper or lower signs are used, respectively, for the lower (n=1) or upper (n=3) regions to insure

that the boundary conditions are met on the bottom and top walls. To determine the expansion coefficients we must enforce the boundary conditions at the dielectric interface and at the inner conductor. At the dielectric interface the tangential fields, E_x, E_z, H_x and H_z must be continuous. This allows the fields in region 2 to be written in terms of the fields in region 1 as follows:

$$\frac{A_{m1}}{A_{m2}} = \frac{\gamma_{mo}}{\gamma_{m1}} \frac{R_{m2}}{\sinh \gamma_{m1}(b-d)} \quad ,$$

$$\frac{B_{m1}}{B_{m2}} = \left[\mu_r \sinh \gamma_{m1}(b-d)\right]^{-1} \quad , \tag{10}$$

$$\frac{A_{m1}}{A_{m2}} = \left[\varepsilon_r \cosh \gamma_{m1}(b-d)\right]^{-1} \quad , \tag{11}$$

and

$$\frac{B_{m1}}{B_{m2}} = \frac{\gamma_{mo}}{\gamma_{m1}} \frac{S_{m2}}{\cosh \gamma_{m1}(b-d)} \quad ,$$

which thus requires that

$$R_{m2} = \varepsilon_r^{-1} \frac{\gamma_{m1}}{\gamma_{mo}} \tanh \gamma_{m1}(b-d)$$

and

$$S_{m2} = \mu_r^{-1} \frac{\gamma_{m1}}{\gamma_{mo}} \coth \gamma_{m1}(b-d) \; .$$

At the inner conductor we require that the electric field be continuous and that the magnetic field be discontinuous due to the surface currents on the inner conductor. If we expand these surface currents using a Fourier superposition, then this last condition can be written as follows:

$$J_x = H_{z3} - H_{z2}\Big|_{y=h} = \sum_{m=0}^{\infty} J_{xm} \cos \sigma_m (x+a) \tag{12}$$

and

$$J_z = H_{x2} - H_{x3}\Big|_{y=h} = \sum_{m=0}^{\infty} J_{zm} \sin \sigma_m (x+a) \tag{13}$$

where J_{xm} and J_{zm} are the Fourier components of the currents yet to be determined. By enforcing continuity of the tangential electric fields at the inner conductor we can write the fields in region 2 in terms of the fields in region 3 as follows:

$$\frac{A_{m2}}{A_{m3}} = - \frac{\sinh \gamma_{mo}(b-h)}{\cosh \gamma_{mo}(d+h)} \left[R_{m2} + \tanh \gamma_{mo}(d+h) \right]^{-1} \tag{14}$$

and

$$\frac{B_{m2}}{B_{m3}} = - \frac{\sinh \gamma_{mo}(b-h)}{\cosh \gamma_{mo}(d+h)} \left[1 + S_{m2} \tanh \gamma_{mo}(d+h) \right]^{-1} . \tag{15}$$

If we now impose conditions (12) and (13) and use (14) and (15) we can express A_{m3} and B_{m3} solely in terms of the Fourier

coefficients J_{xm} and J_{zm} as

$$A_{m3} = -\frac{Z_{1m}(\sigma_m J_{xm} + \Gamma J_{zm})}{\gamma_{mo} \sinh \gamma_{mo}(b-h)} \tag{16}$$

and

$$B_{m3} = -j\frac{Z_{2m}(\Gamma J_{xm} + \sigma_m J_{zm})}{k_o \zeta_o \sinh \gamma_{mo}(b-h)} \tag{17}$$

where

$$Z_{1m} \equiv \frac{j \gamma_{mo}\zeta_o \tanh \gamma_{mo}(b-h)}{k_o(\sigma_m^2 - \Gamma^2)} \left\{ 1 + \tanh \gamma_{mo}(b-h) \left[\frac{1 + R_{m2} \tanh \gamma_{mo}(d+h)}{R_{m2} + \tanh \gamma_{mo}(d+h)}\right]\right\}^{-1} \tag{18}$$

and

$$Z_{2m} \equiv \frac{j k_o\zeta_o \tanh \gamma_{mo}(b-h)}{\gamma_{mo}(\sigma_m^2 - \Gamma^2)} \left\{ 1 + \tanh \gamma_{mo}(b-h) \left[\frac{S_{m2} + \tanh \gamma_{mo}(d+h)}{1 + S_{m2} \tanh \gamma_{mo}(d+h)}\right]\right\}^{-1} \tag{19}$$

Equations (10), (11), (14) and (15), together with (16) and (17) can then be used to express all of the rest of the field components in terms of J_{xm} and J_{zm}.

The remaining boundary condition that must be enforced is that the tangential electric field vanish on the inner conductor. Inserting (8) and (9) into (6) and (7) and evaluating the resulting expressions at the inner conductor, we see that the following

conditions must be met:

$$\sum_{m=0}^{\infty} [(\sigma_m^2 Z_{1m} + \Gamma^2 Z_{2m}) J_{xm} + \Gamma\sigma_m (Z_{1m} + Z_{2m}) J_{zm}] \cos \sigma_m (x+a) = 0 \tag{20}$$

and

$$\sum_{m=0}^{\infty} [\Gamma\sigma_m (Z_{1m} + Z_{2m}) J_{xm} + (\Gamma^2 Z_{1m} + \sigma_m^2 Z_{2m}) J_{zm}] \sin \sigma_m (x+a) = 0 \tag{21}$$

where

$$-w_2 < x < w_1 \quad .$$

The Fourier coefficients of the currents in the above expressions can be found by inverting (12) and (13) as follows:

$$J_{xm} = \frac{\Delta_m}{a} \int_{-w_2}^{w_1} J_x(x') \cos \sigma_m (x'+a) dx'$$

$$= \frac{-2\Delta_m}{\pi m} \int_{-w_2}^{w_1} \partial_{x'} J_x(x') \sin \sigma_m (x'+a) \, dx' \tag{22}$$

and

$$J_{zm} = \frac{1}{a} \int_{-w_2}^{w_1} J_z(x') \sin \sigma_m (x'+a) \, dx' \tag{23}$$

where Δ_m is the Neumann factor defined as

$$\Delta_m = \begin{cases} 1/2 & , \quad m = 0 \\ 1 & , \quad m > 0 \end{cases} .$$

The integrations in (22) and (23) are only over the inner conductor since the currents must vanish outside this range. In (22) we have integrated by parts in order that the unknown $\partial_{x'} J_x(x')$ have the same singularity behavior near the edges of the inner conductor as $J_z(x')$. We can now insert (22) and (23) into (20) and (21) and obtain the following two coupled integral equations for the unknowns $\partial_x J_x$ and J_z :

$$P \int_{-w_2}^{w_1} \partial_{x'} J_x(x') G_{11}(x,x')dx' + P \int_{-w_2}^{w_1} J_z(x') G_{12}(x,x')dx' = 0 \tag{24}$$

and

$$\int_{-w_2}^{w_1} \partial_{x'} J_x(x') G_{21}(x,x')dx' + \int_{-w_2}^{w_1} J_z(x') G_{22}(x,x')dx' = 0 \tag{25}$$

where

$$G_{11} = -\frac{1}{2} \sum_{m=0}^{\infty} \frac{\Delta_m}{\sigma_m} (\sigma_m^2 Z_{1m} + \Gamma^2 Z_{2m}) \cos \sigma_m(x+a) \sin \sigma_m(x'+a) \quad , \tag{26}$$

$$G_{12} = \frac{\Gamma}{a} \sum_{m=0}^{\infty} \sigma_m (Z_{1m} + Z_{2m}) \cos \sigma_m(x+a) \sin \sigma_m(x'+a) \quad , \tag{27}$$

$$G_{21} = -\frac{\Gamma}{a}\sum_{m=0}^{\infty}(Z_{1m} + Z_{2m})\sin\sigma_m(x+a)\sin\sigma_m(x'+a) \quad , \tag{28}$$

$$G_{22} = \frac{1}{a}\sum_{m=0}^{\infty}(\Gamma^2 Z_{1m} + \sigma_m^2 Z_{2m})\sin\sigma_m(x+a)\sin\sigma_m(x'+a) \quad , \tag{29}$$

and P denotes that the integral is to be interpreted in the principal value sense. In order that the kernels of the above two integral equations have the same singularity structure, it is convenient to differentiate (25) with respect to x and obtain

$$P\int_{-w_2}^{w_1} \partial_{x'} J_x(x')\,\partial_x G_{21}(x,x')dx' + P\int_{-w_2}^{w_1} J_z(x')\,\partial_x G_{22}(x,x')dx' = 0 \tag{30}$$

3. EXTRACTION OF THE SINGULAR KERNELS

The kernels given in (26) through (29) can all be written as a sum of two terms; one of which, $\tilde{G}$, is singular for $x = x'$, and the other, $\hat{G} = G - \tilde{G}$, is nonsingular. By extracting the singular parts we can convert (24) and (30) into standard forms of the singular integral equation which can then be inverted exactly. We can identify the singular parts by replacing the coefficients in front of the trigonometric functions in (26) to (29) by their asymptotic forms for large "m". These sums can then be evaluated in closed-form and are given as

$$\tilde{G}_{11} = -\frac{\pi Z_1}{2a^2}\sum_{m=0}^{\infty}\cos m\theta \sin m\phi = -\frac{\pi Z_1}{4a^2}\frac{\sin\phi}{(\cos\theta - \cos\phi)} \quad ,$$

$$\tilde{G}_{12} = -\Gamma\,\tilde{G}_{11} \quad ,$$

$$\tilde{G}_{21} = -\frac{\Gamma Z_1}{a} \sum_{m=1}^{\infty} \frac{\sin m\vartheta \sin m\phi}{m} = -\frac{\Gamma Z_1}{4a} \ln \left| \frac{1 - \cos(\vartheta+\phi)}{1 - \cos(\vartheta-\phi)} \right| \quad ,$$

and

$$\tilde{G}_{22} = -\Gamma(1 + D^{-1})\, \tilde{G}_{21} \quad ,$$

where

$$\vartheta \equiv \frac{\pi}{2a}(x+a) \quad , \tag{31}$$

$$\phi \equiv \frac{\pi}{2a}(x'+a) \quad , \tag{32}$$

$$D = \left(\frac{2a\Gamma}{\pi}\right)^2 \frac{Z_1}{Z_2} \quad ,$$

and Z_1 and Z_2 are respectively the coefficients in the asymptotic expansions of (18) and (19) :

$$Z_{1m} \sim \frac{Z_1}{m}$$

and

$$Z_{2m} \sim \frac{Z_2}{m^3} \quad .$$

The values of Z_1 and Z_2 depend on whether or not the inner conductor is located right on the dielectric interface. Thus,

$$Z_1 = \frac{ja\varsigma_o}{\pi k_o} \quad ,$$

$$Z_2 = \left(\frac{2ak_o}{\pi}\right)^2 Z_1 \quad ,$$

and

$$D = \left(\frac{\Gamma}{k_o}\right)^2 \quad ,$$

if

$$(d+h) \neq 0 \quad ,$$

and

$$Z_1 = \frac{2ja\zeta_o}{\pi k_o(1+\epsilon_r)}$$

$$Z_2 = \left(\frac{2ak_o}{\pi}\right)^2 \left[\frac{1+\epsilon_r}{1+\mu_r^{-1}}\right] Z_1 \quad ,$$

and

$$D = \left(\frac{\Gamma}{k_o}\right)^2 \left[\frac{1+\mu_r^{-1}}{1+\epsilon_r}\right] \quad ,$$

if

$$(d+h) = 0 \quad .$$

The remaining nonsingular correction series are then given as

$$G_{1j} = \sum_{m=1}^{\infty} g_{1j,m} \cos m\theta \sin m\phi - \frac{\Gamma^2}{\pi} Z_{20}\phi \, \delta_{1j} \quad , \qquad j = 1,2$$

and

$$\hat{G}_{2j} = \sum_{m=1}^{\infty} g_{2j,m} \sin m\theta \sin m\phi , \qquad j = 1,2$$

where

$$g_{11,m} = -\frac{1}{a}\left[\frac{1}{\sigma_m}(\sigma_m^2 Z_{1m} + \Gamma^2 Z_{2m}) - \frac{\pi Z_1}{2a}\right]$$

$$g_{12,m} = \frac{\Gamma}{a}\left[\sigma_m(Z_{1m} + Z_{2m}) - \frac{\pi Z_1}{2a}\right] ,$$

$$g_{21,m} = -\frac{\Gamma}{a}\left[(Z_{1m} + Z_{2m}) - \frac{Z_1}{m}\right] ,$$

and

$$g_{22,m} = \frac{1}{a}\left[(\Gamma^2 Z_{1m} + \sigma_m^2 Z_{2m}) - \frac{\Gamma^2 Z_1}{m}(1+D^{-1})\right] .$$

4. SOLUTION OF THE COUPLED EQUATIONS

Having extracted the singular kernels, we can now move the nonsingular corrections series to the right-hand sides of the integral equations given in (24) and (30) and treat these as forcing terms. Transforming to the variables θ and ϕ defined respectively in (31) and (32) we then find the following:

$$P\int_{\phi_1}^{\phi_2} f_1 \tilde{G}_{11} d\phi = -\int_{\phi_1}^{\phi_2} \{[D(f_1-f_2) + f_1]\hat{G}_{11} + \frac{D}{\Gamma}(f_1-f_2)\hat{G}_{12}\} d\phi \tag{33}$$

and

$$P\int_{\phi_1}^{\phi_2} f_2 \partial_\theta \tilde{G}_{21} d\phi = -\int_{\phi_1}^{\varphi_2} \{[D(f_1-f_2) + f_1]\partial_\theta \hat{G}_{21}$$

$$+ \frac{D}{\Gamma}(f_1-f_2)\partial_\theta \hat{G}_{22}\} \, d\phi \qquad (34)$$

where

$$f_1(\phi) \equiv \partial_{x'} J_x(x') - \Gamma J_z(x') \ ,$$

$$f_2(\phi) \equiv \partial_{x'} J_x(x') - \Gamma(1 + D^{-1}) J_z(x') \ ,$$

$$\phi_1 = \frac{\pi}{2a}(a - w_2) \ ,$$

$$\phi_2 = \frac{\pi}{2a}(a + w_1) \ ,$$

and P denotes a principal value integral. We now invoke Schwinger's transformation:

$$\cos\theta = \alpha - \beta v$$

and

$$\cos\phi = \alpha - \beta u$$

with α and β given by

$$\alpha = \frac{1}{2}[\cos\phi_1 + \cos\phi_2]$$

and

$$\beta = \frac{1}{2}[\cos\varphi_1 - \cos\phi_2]$$

in order to transform (33) and (34) into canonical forms of the singular integral equation:

$$T_v[F_i(u)] = H_i(v) \quad , \quad i = 1,2$$

where

$$T_v[F_i(u)] = \frac{1}{\pi} P \int_{-1}^{1} \frac{F_i(u)}{u-v} \, du$$

with

$$F_1(u) = f_1(\phi) \ ,$$

$$F_2(u) = f_2(\phi) \ ,$$

$$H_1(v) = \left(\frac{2a}{\pi}\right)^2 \frac{1}{Z_1} \int_{\phi_1}^{\phi_2} \{[D(f_1-f_2) + f_1] \hat{G}_{11} + \frac{D}{\Gamma}(f_1-f_2) \hat{G}_{12}\} \, d\phi \tag{35}$$

and

$$H_2(v) = \frac{2a}{\pi\Gamma Z_1} \int_{\phi_1}^{\phi_2} \{[D(f_1-f_2) + f_1]\partial_\theta \hat{G}_{21} + \frac{D}{\Gamma}(f_1-f_2)\partial_\theta \hat{G}_{22}\} \, d\phi \ . \tag{36}$$

Again, we expand $H_i(v)$ into a series of Chebyshev polynomials of the second kind U_m as

$$H_i(v) = \sum_{m=0}^{\infty} C_{m+1,i} U_m(v) \tag{37}$$

and use the following identity:

$$F_i(v) = (1-v^2)^{-1/2}\{C_{oi} - T_v[(1-u^2)^{1/2}H_i(u)]\}$$

together with:

$$T_v[(1-u^2)^{1/2}U_m(u)] = -T_{m+1}(v)$$

to solve for $F_i(v)$ as

$$F_i(v) = (1-v^2)^{-1/2} \sum_{m=0}^{\infty} C_{mi}T_m(v) , \quad i = 1,2 \tag{38}$$

where $T_m(v)$ is a Chebyshev polynomial of the first kind and the expansion coefficients C_{mi} are as yet to be determined.

5. SECULAR EQUATION FOR A TEM-CELL WITH A DIELECTRIC SLAB

In order to complete the solution given in (38) it is necessary to evaluate the constants C_{mi}. As shown in [19], an infinite set of equations for the C_{mi}'s can be derived by substituting the expressions for F_i and H_i given respectively in (38) and (37) into the defining equations (35) and (36) and matching coefficients of $U_m(v)$. Two additional equations are also needed. These are found by substituting the solution for F_i into the initial undifferentiated integral equation (25), and by equating the longitudinal current components obtained from the solutions of (24) and (30). (In so doing, the requirement that the transverse current component vanish at the edges of the inner conductor is enforced.) The equations that result are given as

follows:

$$C_{n+1,1} = \frac{2a\delta}{\pi Z_1} \sum_{m=n}^{\infty} \sum_{k=0}^{m-1} (1-\delta_{mo}) q_{nm} \frac{p_{k,m-1}}{\Delta_k} \{[(1+D)g_{11,m} + \frac{D}{\Gamma} g_{12,m}]C_{k1}$$

$$- D[g_{11,m} + \frac{1}{\Gamma} g_{12,m}] C_{k2}\} \quad n = 0,1,2,\ldots , \qquad (39)$$

$$C_{n+1,2} = \frac{a\beta}{\Gamma Z_1} \sum_{m=n}^{\infty} \sum_{k=0}^{m-1} (1-\delta_{mo}) q_{nm} \frac{p_{k,m-1}}{\Delta_k} \{[(1+D)g_{21,m} + \frac{D}{\Gamma} g_{22,m}]C_{k1}$$

$$- D[g_{21,m} + \frac{1}{\Gamma} g_{22,m}] C_{k2}\} \quad n = 0,1,2,\ldots , \qquad (40)$$

$$\sum_{n=0}^{\infty} C_{n2} J_n = \frac{2a}{\Gamma Z_1} \sum_{n=0}^{\infty} \sum_{k=0}^{n} \frac{p_{kn}}{\Delta_k} \cos(\frac{n\pi}{2}) \{g_{21,n+1}[(1+D)C_{k1} - DC_{k2}]$$

$$+ \frac{D}{\Gamma} g_{22,n+1}(C_{k1} - C_{k2})\} , \qquad (41)$$

$$\sum_{n=0}^{\infty} C_{n2} I_n = (1+D^{-1}) \sum_{n=0}^{\infty} C_{n1} I_n , \qquad (42)$$

where δ_{mo} is the Kronecker delta, Δ_k is the Neumann factor, p_{mn} and q_{mn} are, respectively, the expansion coefficients of $\sin(n+1)\phi/\sin\phi$ and $\cos n\phi$ in terms of Chebyshev polynomials $T_m(u)$ and $U_m(u)$ with $u = (\alpha-\cos\phi)/\beta$, and I_n and J_n are the canonical integrals which are evaluated in [19].

The solution of the above set of equations determines the propagation constant Γ . Although (39) through (42) represent an infinite matrix equation for the C_{mi}'s , it is possible to truncate this set of equations to one of very small order since the

coefficients $g_{ij,m}$ of the nonsingular kernels, in most cases, converge extremely rapidly with "m".

In the following, we will assume that $C_{n1} = C_{n2} = 0$ for $n > 0$ so that the infinite matrix equation reduces to just a simple 2x2 matrix. This approximation places some restrictions on the various dimensions of the stripline which one can allow and still obtain accurate values for the propagation constant.

The nature of this approximation can best be understood by examining the form of the current as given by (38). The dominant feature of this solution is contained in the factor $(1-v^2)^{-1/2}$ which governs the behavior near the sharp edges of the inner conductor. The remaining Chebyshev expansion tailors the distribution away from the edges. The constant part of this expansion is retained in the 2x2 matrix approximation. In most cases, one would expect this to represent the exact distribution fairly accurately. This would not be the case, however, when one of the following occurs: (1) either the top or bottom wall of the outer conductor approaches the inner conductor, (2) the dielectric layer is close to but not quite touching the inner conductor, (3) the inner conductor is located at the dielectric interface and is relatively wide compared to the width of the dielectric layer, or (4) one is interested in a higher-order mode with a large cutoff frequency.

The limitation encountered with the first of the above cases is analogous to that which was found earlier for the RCTL without dielectric [16]. The approximate solution breaks down for small b/a (i.e., when the inner conductor is close to the top and bottom walls of the outer conductor).

The reason for the restriction in the second case mentioned above can best be seen by examining the expressions for Z_{1m} and Z_{2m} as given, respectively, in (18) and (19). In extracting the asymptotic forms of these expressions for large "m" we obtained two different results depending upon whether or not $(d+h) = 0$. When $(d+h)$ was close to but not quite zero (i.e., the dielectric layer was near the inner conductor) then a larger value of "m" was needed in order to make $\tanh \gamma_{mo}(d+h)$ approach 1. Therefore, since the nonsingular kernels do not converge as rapidly, the 2×2 approximation breaks down. When the inner conductor is exactly on the interface, the 2×2 approximation is again quite accurate as the correct asymptotic form was extracted (i.e., $\tanh \gamma_{mo}(d+h) \to 0$).

In the third case, one would expect the current distribution to approach that of a parallel stripline formed by the inner conductor and its image about the bottom wall of the outer conductor. Since we know that the current distribution in this case is significantly different from that predicted by (38), again the 2×2 approximation breaks down.

Finally, for very high-order modes, the expressions for Z_{1m} and Z_{2m} do not converge very rapidly, and the 2×2 approximation breaks down.

Summarizing the above restrictions, we can say that for the dominant mode and the first few higher-order modes, one would expect the 2×2 approximation to be quite accurate as long as the inner conductor is not too close to either the top or bottom walls of the outer conductor or the dielectric layer. As will be demonstrated, very accurate results for the propagation constants can be obtained assuming this rather simplified current distirbution. This should not be too surprising since we know that a variational expression for the propagation constant can be formulated which is not too sensitive to the exact distribution used for the current.

The secular equation for the 2x2 approximation can be found from (41) and (42) as

$$(1+D) = \frac{S_o}{J_o} \tag{43}$$

where

$$S_o = -\frac{4aD}{\Gamma^2 Z_1} \sum_{m=0}^{\infty} p_{on} \cos\left(\frac{n\pi}{2}\right) g_{22,n+1}$$

and J_o, as derived in [19] is given by

$$J_o = \frac{2k}{\sqrt{\beta}} K(k') \tag{44}$$

with

$$k = \left[\frac{4\beta}{(1+\beta^2)-\alpha^2}\right]^{1/2} ,$$

$$k' = [1-k^2]^{1/2} ,$$

and $K(k')$ is a complete elliptic integral of modulus k'. For simplicity, we will assume that the inner conductor is symmetrically located about the y-axis (i.e., $\alpha=0$) so that we can apply Gauss' transformation to (44) and obtain

$$J_o = 2K(\beta') . \tag{45}$$

Before we present any numerical data from the solution of (43), it is instructive to examine some limiting cases which can

be obtained analytically. In the case of a narrow center septum, the canonical integral J_o given in (45) can be further simplified by replacing it with its asymptotic form for modulus near one:

$$J_o \sim 2 \ln \frac{4}{3} = 2 \ln \left[\frac{4}{\sin\left(\frac{\pi w}{2a}\right)} \right] \tag{46}$$

As the septerm width becomes exceedingly small one can see from (46) that (43) will reduce to

$$(1+D) = 0$$

which can be solved to give

$$\Gamma = \begin{cases} jk_o & , \; d+h \neq 0 \\ jk_o \left[\dfrac{1+\varepsilon_r}{1+\mu_r^{-1}} \right]^{1/2} & , \; d+h = 0 \end{cases} \tag{47}$$

Equation (47) for $d+h = 0$ is Coleman's well-known narrow-strip result [17] in which the effective dielectric constant is just the average of the dielectric constants above and below the inner conductor.

Another case that might be of interest is the static limit. In this case (43) is no longer a transcendental function of Γ and can be solved explicitly for the propagation constant. Furthermore, if the inner conductor is located at the dielectric interface and is also symmetrically located within the inner conductor, one can show that the static propagation constant is given by

that in (47) for $d + h = 0$ independent of the width of the inner conductor. As shown in [18] this is an exact result of the related problem where the side walls are removed to infinity when the dielectric layer fills exactly half the guide.

As a final comment one can easily show that $\Gamma = jk_o$ is a solution to (43) in the trivial case when $\varepsilon_r = \mu_r = 1$, since $g_{22,n} = 0$ when $\Gamma = jk_o$.

6. NUMERICAL RESULTS AND CONCLUDING REMARKS

The roots of the secular equation given in (43) were calculated using a bisection subroutine. If the frequency is high enough then more than one root may exist, indicating the presence of higher-order modes. We will first, however, restrict attention to just the dominant mode. In addition, unless otherwise stated, the following data will apply for the case of a non-elevated inner conductor located symmetrically about the y-axis. Shown in Table 1 are the calculated propagation constants of the dominant mode of a stripline structure at three different frequencies. The dimensions of this stripline are the same as those used by Mittra and Itoh [10] and Hornsby and Gopinath [3], and their results are included for comparison.

TABLE 1

COMPARISON OF THE PROPAGATION CONSTANT $\Gamma/j = k_o\beta_o (mm^{-1})$

OBTAINED BY DIFFERENT METHODS FOR $\varepsilon_r = 9.$, $\mu_r = 1.$,

$a = 1.75$ mm, $b = 1$ mm, $d = -h = .5$ mm, $w_1 = w_2 = .5$ mm

Frequency (GHz)	Mittra and Itoh [10]	Hornsby and Gopinath [3]	Solution of (43)
10	0.53	0.55	0.54
20	1.10	1.17	1.13
30	1.71	1.77	1.76

Figure 2 shows the effective dielectric constant for a dielectric loaded RCTL of dimensions corresponding to a typical TEM cell [16]. The inner conductor is symmetrically located within the outer conductor and the width of the dielectric layer is varied by changing the parameter d/b. As can be seen, for normalized widths of the dielectric layer d/b less than 0.2, the propagation constant of the dominant mode is very close to jk_o, and very little dispersion is evident since the dispersion curves are very flat over a wide range in frequency. The same data are presented in an alternate form in Fig. 3. In this figure the abscissa is d/b and the parameter $k_o a$ is varied. These curves give an indication of how narrow the width of the dielectric layer must be in order that the dominant mode is essentially TEM (i.e., $\Gamma = jk_o$).

In the previous two figures, the dielectric was assumed to be lossless. We will now introduce some loss in the dielectric by replacing ε_r by $\varepsilon_r(1-j \tan \delta)$ where $\tan \delta$ is the loss tangent. In this way we hope to model the lossy absorbing material which is sometimes placed inside a TEM cell to cut the Q of the higher-order modes and thus extend the cell's useful frequency range. The propagation constant will now be complex and we will define the normalized complex propagation constant as $\Gamma/jk_o = \beta_o - j\alpha_o$ where β_o is the normalized propagation constant and α_o is the normalized attenuation constant. In Fig. 4 and 5, respectively, we plot β_o and α_o as a function of the normalized frequency for a dielectric with $\varepsilon_r = 4$ and a loss tangent of 0.25. The important thing to note in Fig. 5 is that the attenuation constant for the dominant mode is the same order of magnitude as the first two higher-order modes for frequencies just above the cutoff frequency of the first higher-order mode. Thus, at first sight,

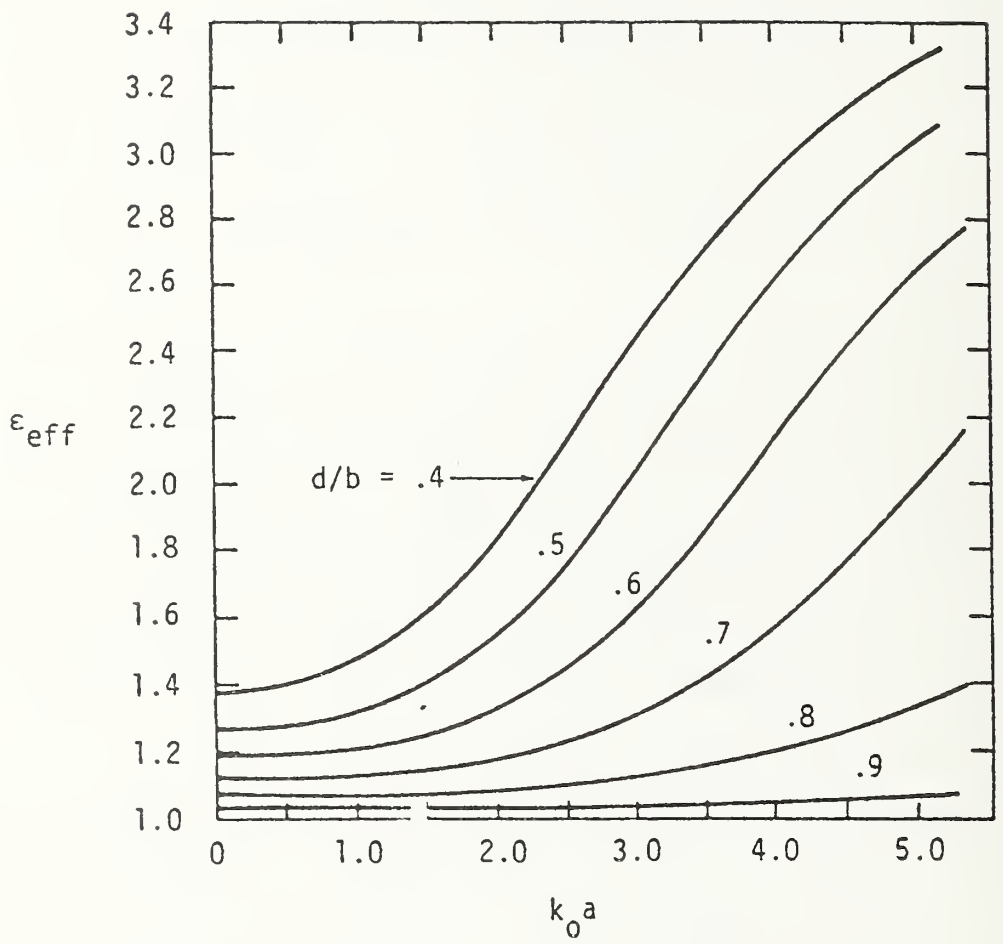

Fig. 2. Effective dielectric constant of the dominant mode vs. normalized frequency for a dielectric-loaded RCTL with parameters:
$\varepsilon_r = 4.$, $\mu_r = 1.$ $b/a = .6$, $h/b = 0.$, $w_1/a = w_2/a = .72.$

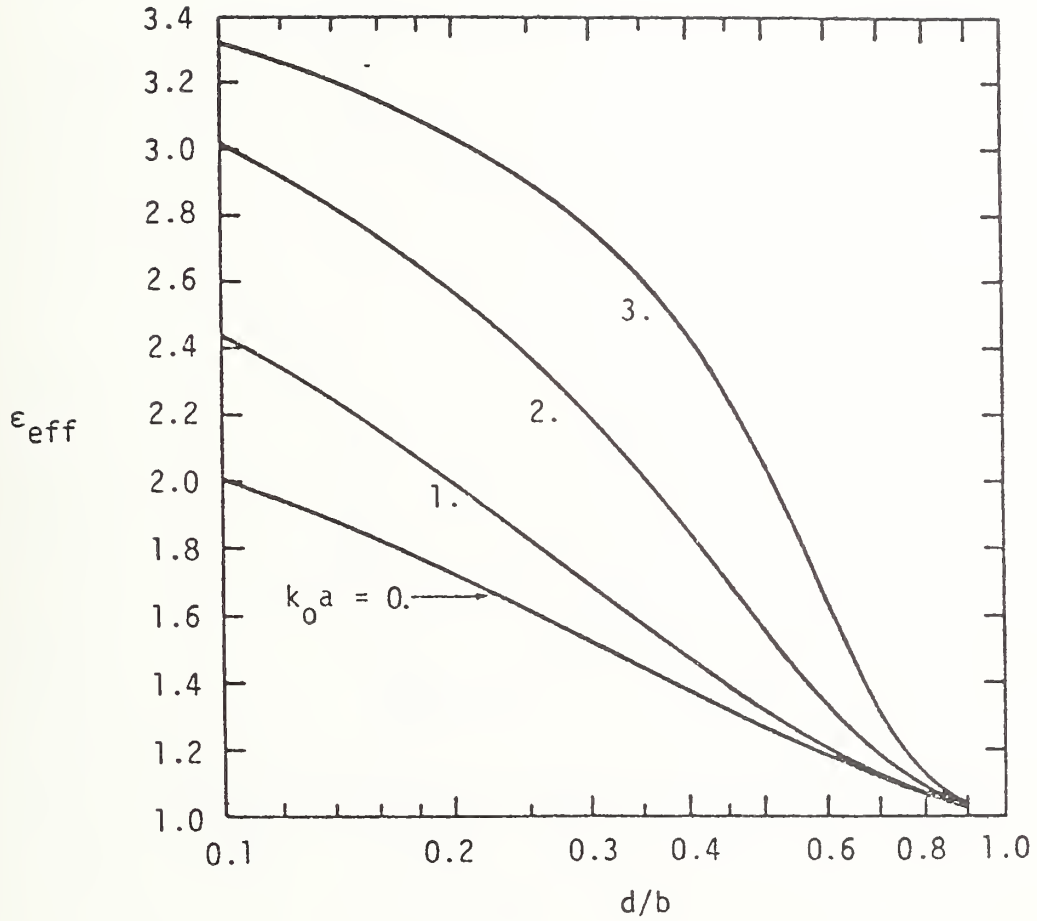

Fig. 3. Effective dielectric constant of the dominant mode vs. d/b for a dielectric-loaded RCTL with parameters: $\varepsilon_r = 4.$, $\mu_r = 1.$, $b/a = .6$, $h/b = 0.$, $w_1/a = w_2/a = .72$.

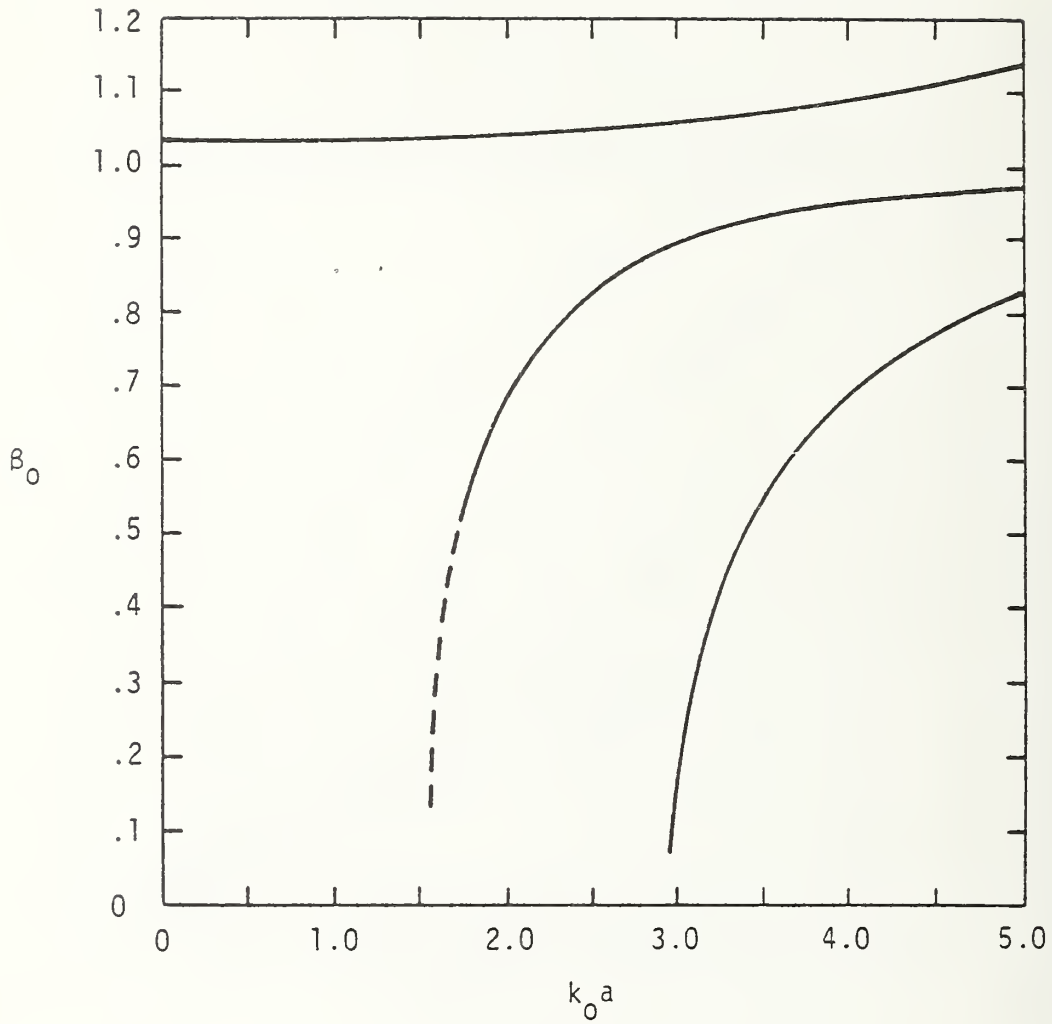

Fig. 4. Normalized propagation constant of the dominant and first two higher-order modes vs. normalized frequency for an RCTL loaded with a lossy dielectric and having parameters:
$\varepsilon_r = 4.$, $\mu_r = 1.$, $\tan\delta = .25$, $b/a = .6$, $h/b = 0.$, $d/b = .8$, $w_1/a = w_2/a = .72$.

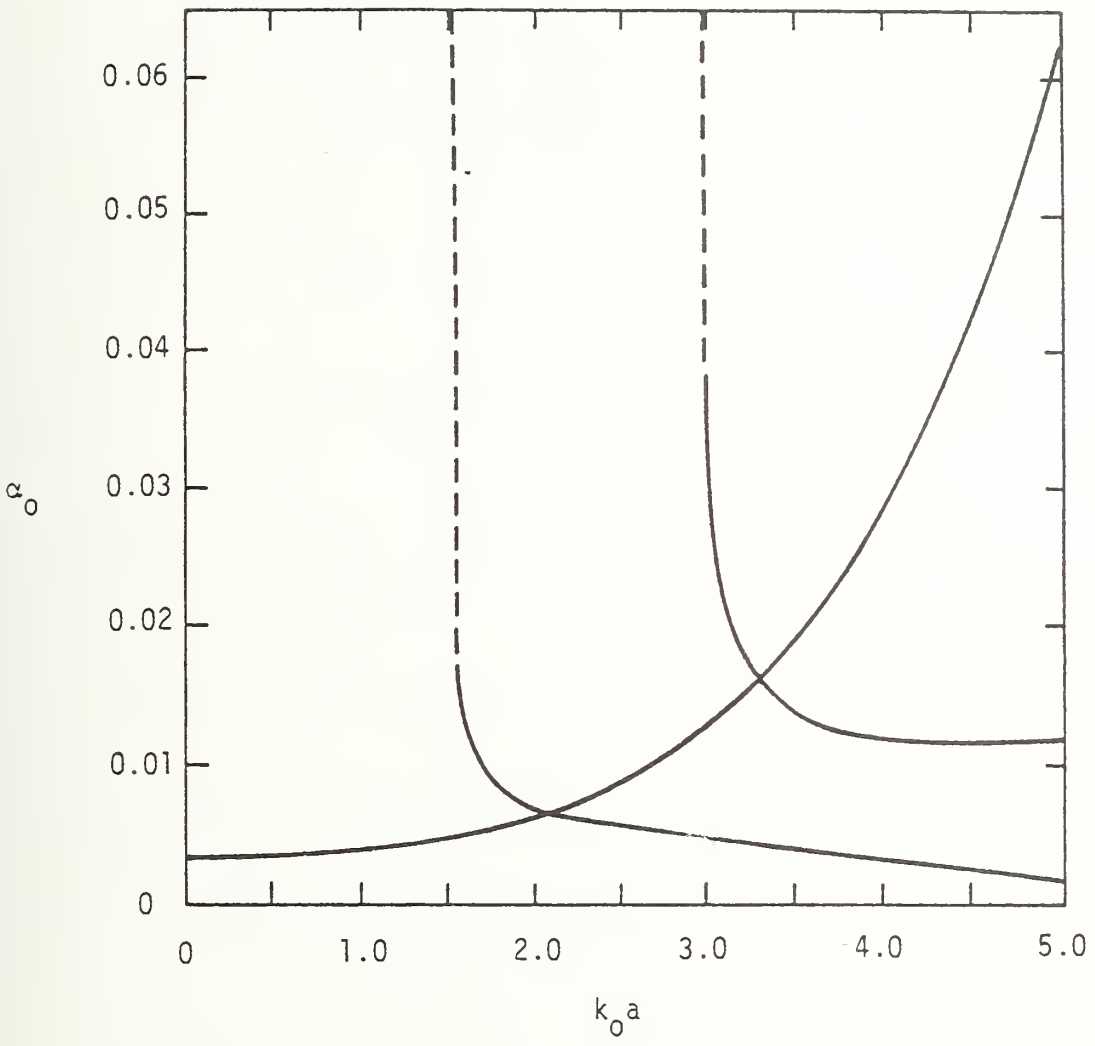

Fig. 5. Normalized attenuation constant of the dominant and first two higher-order modes vs. normalized frequency for an RCTL loaded with a lossy dielectric and having parameters:
$\varepsilon_r = 4.$, $\mu_r = 1.$, $\tan\delta = .25$, $b/a = .6$, $h/b = 0.$,
$d/b = .8$, $w_1/a = w_2/a = .72$.

it would appear that the lossy dielectric layer does not act as a very good mode filter. However, for an absorber loaded TEM cell, one must remember that the RCTL is terminated in two tapered sections which represent reactive loads on the transmission line. Thus, from a resonance standpoint, the introduction of a small amount of loss in the propagation constant of the higher-order modes could substantially reduce the Q of these modes without adversely affecting the dominant TEM mode.

7. REFERENCES

[1] M.L. Crawford, J.L. Workman and C.L. Thomas, "Expanding the bandwidth of TEM cells for EMC measurements," IEEE Trans. EMC. vol. 20, no. 3, pp. 368-375, Aug. 1978.

[2] H.E. Stinehelfer, Sr., "An accurate calculation of uniform microstrip transmission lines," IEEE Trans. Microwave Theory Tech., vol. MTT-16, pp. 439-444, July 1968.

[3] J.S. Hornsby and A. Gopinath, "Numerical analysis of a dielectric-loaded waveguide with a microstrip line-finite-difference methods," IEEE Trans. Microwave Theory Tech., vol. MTT-17, pp. 684-690, Sept. 1969.

[4] D.G. Corr and J.B. Davies, "Computer analysis of the fundamental and higher-order modes in single and coupled microstrip," IEEE Trans. Microwave Theory Tech., vol. MTT-20, pp. 669-677, Oct. 1972.

[5] P. Daly, "Hybrid-mode analysis of microstrip by finite-element methods," IEEE Trans. Microwave Theory Tech., vol. MTT-19, pp. 19-25, Jan. 1971.

[6] L.N. Deryugin, O.A. Kurdyumov, and V.E. Sotin, "Fundamental and parasitic wave modes of a shielded microstrip line," Radiophys. Quantum Electron., vol. 16, pp. 89-96, Jan. 1973.

[7] M.K. Krage and G.I. Haddad, "Frequency-dependent characteristics of microstrip transmission lines," IEEE Trans. Microwave Theory Tech., vol. MTT-20, pp. 678-688, Oct. 1972.

[8] J. Dekleva and V. Roje, "Modovi oklopljene mikrostrip linije," Elektrotehnika (Zagreb), vol. 18, pp. 293-296, 1975.

[9] Y. Fujiki, T. Kitazawa and M. Suzuki, "Analysis of higher-order modes in single, coupled and asymmetrical striplines," Electron. Commun. in Jap., vol. 57-B, pp. 89-95, Oct. 1974.

[10] T. Itoh and R. Mittra, "A technique for computing dispersion characteristics of shielded microstrip lines," IEEE Trans. Microwave Theory Tech., vol. MTT-22, pp. 896-898, Oct. 1974.

[11] R. Jansen, "Zur numerischen berechnung geschirmter streifenleitungs-strukturen," Arch. Elek. Übertragung., vol. 29, pp. 241-247, June 1975.

[12] G. Kowalski and R. Pregla, "Dispersion characteristics of shielded microstrips with finite thickness," Arch. Elek. Übertragung., vol. 25, pp. 193-196, Apr. 1971.

[13] R. Mittra and T. Itoh, "A new technique for the analysis of the dispersion characteristics of microstrip lines," IEEE Trans. Microwave Theory Tech., vol. MTT-19, pp. 47-56, Jan. 1971.

[14] G. Essayag and B. Sauve, "Effects of geometrical parameters of a microstrip on its dispersive properties," Electron. Lett., vol. 8, pp. 529-530, Oct. 1972.

[15] G. Essayag and B. Sauve, "Study of higher-order modes in a microstrip structure," Electron. Lett., vol. 8, pp. 564-566, Nov. 1972.

[16] J.C. Tippet and D.C. Chang, "Properties of a rectangular cross-section transmission line with an offset inner conductor," accepted for publication in IEEE Trans. Micrw. Theory and Tech., vol. MTT-27, 1979.

[17] B.L. Coleman, "Propagation of electromagnetic disturbances along a thin wire in a horizontally stratified medium," Phil. Mag., vol. 41, ser. 7, pp. 276-288, Mar. 1950.

[18] G. Kowalski and R. Pregla, "Calculation of the distributed capacitances of coupled microstrips using a variational integral," Arch. Elek. Übertragung., vol. 27, pp. 51-52, Jan. 1973.

[19] J.C. Tippet, Modal characteristics of rectangular coaxial transmission-line, Ph.D. Thesis, Department of Electrical Engineering, University of Colorado, Boulder, CO, 1978.

ACKNOWLEDGMENT

The authors are indebted to Professors L. Lewin and E.F. Kuester, University of Colorado; Professor M.T. Ma and Mr. M. Crawford, NBS Boulder Laboratories, for their very useful comments and suggestions. The work is supported under Contract No. CST-8447.

NBS-114A (REV. 9-78)

U.S. DEPT. OF COMM. BIBLIOGRAPHIC DATA SHEET	1. PUBLICATION OR REPORT NO. NBSIR 79-1615	2. Gov't. Accession No.	3. Recipient's Accession No.

4. TITLE AND SUBTITLE

Dispersion and Attenuation Characteristics of Modes in a TEM-Cell with a Lossy Dielectric Slab

5. Publication Date

August 1979

6. Performing Organization Code

7. AUTHOR(S)

John C. Tippet and David C. Chang

8. Performing Organ. Report No.

9. PERFORMING ORGANIZATION NAME AND ADDRESS

Department of Electrical Engineering
University of Colorado
Boulder, Colorado 80309

10. Project/Task/Work Unit No.

11. Contract/Grant No.

CST-8447

12. SPONSORING ORGANIZATION NAME AND COMPLETE ADDRESS *(Street, City, State, ZIP)*

National Bureau of Standards
Electromagnetic Fields Division (723)
Boulder, Colorado 80303

13. Type of Report & Period Covered

14. Sponsoring Agency Code

15. SUPPLEMENTARY NOTES

☐ Document describes a computer program; SF-185, FIPS Software Summary, is attached.

16. ABSTRACT *(A 200-word or less factual summary of most significant information. If document includes a significant bibliography or literature survey, mention it here.)*

Dispersion and attenuation characteristics of the dominant mode in a TEM cell, loaded with a lossy dielectric slab, are investigated. It is shown that, while the insertion of the lossy material can indeed lower the Q-factor of the higher-order modes, the attenuation of the dominant mode also increases drastically as frequency increases. Correction to that effect must be taken before measurements in the cell are used to correlate to those taken in a free-space environment.

17. KEY WORDS *(six to twelve entries; alphabetical order; capitalize only the first letter of the first key word unless a proper name; separated by semicolons)*

Attenuation; coupled integral equations; dispersion; lossy dielectric slab; modes considerations; TEM-cell

18. AVAILABILITY

☒ Unlimited

☐ For Official Distribution. Do Not Release to NTIS

☐ Order From Sup. of Doc., U.S. Government Printing Office, Washington, DC 20402, SD Stock No. SN003-003-

☒ Order From National Technical Information Service (NTIS), Springfield, VA. 22161

19. SECURITY CLASS (THIS REPORT)	21. NO. OF PRINTED PAGES
UNCLASSIFIED	36
20. SECURITY CLASS (THIS PAGE)	**22. Price**
UNCLASSIFIED	$4.00

☆ U.S. GOVERNMENT PRINTING OFFICE: 1979-0-677-072/1300 USCOMM-DC

NBSIR '79-1615